Restorative Capacity Optimization for Complex Infrastructure Networks

Nazanin Morshedlou, Kash Barker, *Member, IEEE,* Giovanni Sansavini, *Member, IEEE*

***Abstract*—This research focuses on the planning and scheduling of restoration efforts provided by infrastructure networks in the aftermath of disruptive events. Two mathematical formulations are presented to assign restoration crews to disrupted components and maximize network resilience progress in any given time horizon. In the first formulation, the number of assigned restoration crews to each component can vary to increase the flexibility of models in the presence of different disruption scenarios. Along with considering the assumptions of the first formulation, the second formulation models the condition where the disrupted components can be partially active during the restoration process. We test the efficacy of our formulations on the realistic data set of 400-kV French electric transmission network and 32 realistic size data sets illustrating scale-free, small-world, lattice, and random networks. The results indicate that the proposed formulations can be used for a wide variety of infrastructure networks and for real-time restoration process planning.**

***Index Terms*— Infrastructure networks, network resilience, scale-free networks, small-world networks, scheduling**

I. Introduction and Motivation

THE United States, as well as many countries around the globe, have increasingly emphasized resilience planning for critical infrastructure networks. Presidential Policy Directive 21[1] states that such networks "must be secure and able to withstand and rapidly recover from all hazards." The combination of withstanding and recovering these critical infrastructure networks is generally referred to as *resilience*, formally defined as the "ability to withstand, adapt to, and recover from a disruption"[2]. Examples of critical infrastructure networks include water, gas, communication, transportation, and the electric power grid.

U.S. resilience planning documents highlight terrorist attacks, natural disasters, and manmade hazards, all of which could exacerbate our aging and vulnerable infrastructure systems. The state of these critical infrastructure networks, combined with the fact that climate change will likely result in more frequent, severe, and complicated catastrophic events, motivates planning for resilient infrastructure networks so that they may be recovered quickly after a disruptive event.

There have been many recent attempts to define, model, and measure resilience across a number of application areas[3], including infrastructure networks (e.g., transportation, electric power, pipelines)[4]-[7],and service networks (e.g., emergency response, humanitarian relief, debris removal)[8]-[12]. Fig. 1 offers a paradigm for the resilience of a network prior, during, and in the aftermath of a disruptive event, e^j [14]-[16]. The performance of the network is measured with $\varphi(t)$ (e.g., the extent to which demand is met in an electric power network). The resilience of a network over time is measured with $\mathcal{R}_{\varphi}(t|e^j)$, or the proportion of network performance in each time period after disruption (i.e., $\varphi(t)$ for $t = t_e, \dots, t_f$, caused by disruption scenario, $e^j \in D$ for $D = \{1, \dots, J\}$ where D is a set of possible disruptive events), to network performance prior to the disruption.

Fig. 1 highlights two primary dimensions of resilience: (i) vulnerability, or the lack of ability of a network to maintain its level of performance given the occurrence of a disruptive event, and (ii) recoverability, or the ability of a network to recover to a desired level of performance timely. Vugrin and Camphouse[17] introduced *resilience capacity*, as a function of *absorptive capacity* (i.e., the extent to which a network can absorb disturbances during the occurrence of a disruptive event), *adaptive capacity* (i.e., the extent to which a network can quickly adapt in the aftermath of a disruptive event by short-term, temporary means), and *restorative capacity* (i.e., the extent to which a network can be restored from a disruptive event over a longer time horizon). In Fig. 1, absorptive and adaptive capacity address network vulnerability mitigation, or how to extend the performance (i.e., stable original state) and how to reduce the drop in performance (i.e., system disruption state), respectively. Network recoverability can be addressed with restorative capacity, or how to reduce the time horizon in which restorative operations occur, thus increasing the slope of performance[18].

This paper focuses on enhancing recoverability through restorative capacity. In this area, considerable research in recent years has focused on optimization models and algorithms to improve recovery operations. Recent reviews by Anaya-Arenas et al.[20] and Ozdamar and Ertem[21] discuss post-disruption

This work was supported in part by the National Science Foundation, Division of Civil, Mechanical, and Manufacturing Innovation, under Award 1635813.

N. Morshedlou is with the School of Industrial and Systems Engineering, University of Oklahoma, Norman, OK 73019 USA (e-mail: nazanin.morshedlou@ou.edu).

K. Barker is with the School of Industrial and Systems Engineering, University of Oklahoma, Norman, OK 73019 USA (e-mail: kashbarker@ou.edu).

G. Sansavini is with the Reliability and Risk Engineering Laboratory, Institute of Energy Technology, Department of Mechanical and Process Engineering, ETH Zurich, Zurich, Switzerland (e-mail: sansavig@ethz.ch).

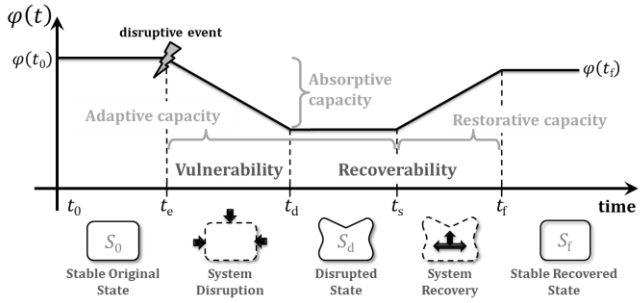

Fig. 1. Relationship between resilience capacities and the primary dimensions of resilience proposed in [14].

restoration plans particularly in humanitarian logistics, such as relief delivery, casualty transportation, and mass evacuation. As far as transportation networks are concerned, Kasaei and Salman[19] study arc routing problems to regain network connectivity by clearing blocked roads, developing heuristic algorithms to attain maximum benefit gained by network connectivity while minimizing the time horizon. Aksu and Ozdamar[22] consider a multi-vehicle problem to maximize network accessibility during transportation network recovery by identifying critical blocked links and restore them with limited resources. Nurre et al.[5] introduce a design and scheduling formulation to expedite the infrastructure network restoration process.

Electric power networks behave differently than transportation networks, as according to laws of physics, power flow cannot be controlled and affected directly. Bienstock and Mattia[4] proposed a mixed integer model to protect power grid networks at minimum costs to increase their survivability to cascading failures. Later Nurre et al.[5] incorporate the method by Bienstock and Mattia[4] to propose a schedule and design problem that models restoration efforts associated with power networks. Fang and Sansavini[23] co-optimize power grid expansion and installation of line switching devices to mitigate the supply disservice in the aftermath of disruptions and enhance resilience by system re-configurability. Xiao and Yeh[25] use a dual covering graph in which nodes represent links in the corresponding original graph and present a model to assess the existence and non-existence of operational links after the failure of degree dependent links. Arif et al.[27] propose a two stage method which first clusters the disrupted lines and grids based on their distance from the restoration depot and then proposes a mixed integer linear program to schedule restoration crews to disrupted locations and dispatch them through the network to minimize the total restoration time. Chen et al.[29][28] introduce a sequential service restoration framework to optimize the restoration process for large-scale power outages, disrupted distribution networks, and microgrids. The framework is formulated as a mixed integer linear program and schedules a set of control actions that synchronize distributed generators, switches, and switchable loads and form multiple isolated microgrids in three-phase unbalanced distribution systems and microgrids.

Many infrastructure networks can be described by models of complex networks (e.g., scale-free and small-world networks), therefore recent research has focused on how network structures facilitate and constrain network behavior, particularly in the aftermath of a disruptive event[29]. Ouyang et al.[30] investigate how the resilience of redundant systems in scale-free networks plays a significant role to reduce the adverse effects of disruptions. Chang and Wu[24] analyze complex network theories and characteristics to be able to track the mechanism of cascading failure, showing that network reliability could decline to 5% as the result of cascading failure. Albert et al.[31] assess level of robustness and vulnerability of complex networks for different disruption scenarios. They show that the malfunction of key components may nevertheless lead to an adverse loss in the complex networks as the result of redundant connections existing in the network structure.

While the aforementioned works deal with various aspects of infrastructure networks after a disruptions, none consider the role of network structure (mesh, random, scale-free, small-world) in planning the restoration process, and none present a framework that can adapt to a variety of infrastructure networks, each with particular performance characteristics. Therefore, we indicate the applicability of the proposed model to a variety of infrastructure networks and study the behavior of the model in presence of different network structure (e.g., from mesh network to scale-free and small-world networks).

Aside from introducing the Binary Active model, in which a disrupted component must be fully recovered to be fully operational (e.g., an electric power line), this paper presents the Proportional Active model, in which a disrupted component can be partially operational in the network while it is being recovered. In the context of power grid network recovery, this is also the case for redundant components connected in a parallel configuration, in which the components equally share the load. Power lines, busbars, and step-down transformers are often operated by following this logic. The capacity and, consequently, the level of operation associated with each disrupted line increase during restoration. Another contribution of this paper allows for variability in the number of crews required to restore disrupted components, each with special characteristics (e.g., restoration time, and level of disruption).

The remainder of the paper is organized as follows. Section II proposes Binary Active infrastructure mathematical formulations for restoration efforts and update the structure of the model to incorporate proportionally operational components in each time period. Section III provides data generation and computational analyses of the impact of Proportional and Binary Active models on scale-free and small-world networks derived from the 400-kV French electric power transmission network, as well as the French power network itself. We discuss concluding remarks in Section IV.

II. Proposed Optimization Model

Let $G = (N, A)$ be an undirected connected network, where N is the set of nodes and A is the set of links. There is a set of supply nodes $N_+ \subseteq N$, a set of demand nodes $N_- \subseteq N$, and a set of transshipment nodes $N_= \subseteq N$. Each supply node $i \in N_+$ supplies amount o_i in each time period, and each demand node $i \in N_-$ demands amount b_i in each time period. Each link $(i, j) \in A$ has a defined pre-disruption capacity u_{ijt_e} and a pre-

calculated flow value x_{ijt_e} based on the solution to the classic flow problem[32] aiming to satisfy demand nodes $i \in N_-$. Power flow rules are not considered in small-world and scale-free instances as the relevant series reactance values are not known.

Some challenges may arise in studying a power network flow formulation: (i) the nonlinearity and nonconvexity of AC power flow, (ii) the complexity of its solution, particularly when it is integrated with network restoration formulation, and (iii) the fact that the system may have multiple solutions[4]. For the sake of simplicity, we use a DC linear approximation to bypass the aforementioned shortcoming. While such an approximation is a simplification, it has shown to provide a good estimation of the network restoration process after a disruption. Furthermore, eliminating the behavior of power networks (e.g., start-up times for units and pick up of ballast loads) decreases the solution time and complexity[4],[5].

With the application of the DC linear approximation model for the 400kV French transmission network (shown in Appendix A), we are interested in sending the amount of flow from supply nodes to satisfy all demand nodes, respecting the flow capacity of links and supply/demand capacities. There exists an importance weight w_i of each demand node $i \in N_-$.

There is a set of links $A' \subseteq A$ that are affected by the disruptive event at time t_e. Without loss of generality, we can consider inoperable nodes as inoperable links since a node can be split to two nodes and a link. The affected links are scheduled to multiple parallel restoration crews, $k = 1, \dots, K$, where K is the maximum number of work crews that can be assigned to each disrupted link $(i,j) \in A'$. The total number of work crews available for all links is L. Each link $(i,j) \in A'$ has an associated processing time p_{ijk} which depends on the characteristics of that link and the number of restoration crews assigned to it. Without loss of generality, p_{ijk} is an integer parameter for each $(i,j) \in A'$. We also assumed that each recovery task should be processed without interruption.

We evaluate the performance of the network in each time period $t = 1, \dots, T$ by determining the total flow reaching demand nodes, denoted by $\sum_{i \in N_-} \varphi_{it}$. The objective function maximizes the resilience of the infrastructure network at each time t, and consequently over the horizon of the problem. The resilience of the system at time t after disruptive event $e^j\ j \in E$, is captured in the objective function with Eq. (1), where $\sum_{i \in N_-} \varphi_{it_e}$ is the performance of the network before the occurrence of disruptive event (at time t_e from Fig. 1), and $\sum_{i \in N_-} \varphi_{it_d}$ is the performance of the network after disruptive effects have occurred (at time t_d).

$$\Re_\varphi(t|e^j) = \frac{\sum_{i \in N_-} \varphi_{it} - \sum_{i \in N_-} \varphi_{it_d}}{\sum_{i \in N_-} \varphi_{it_e} - \sum_{i \in N_-} \varphi_{it_d}} \tag{1}$$

In this paper, we assume total demand does not change during the horizon of the problem. However, in cases where the total demand changes with time, we could substitute $\sum_{i \in N_-} \varphi_{it_e}$ with $\sum_{i \in N_-} E[\varphi]_{it}$, where parameter $E[\varphi]_{it}$ would represent the expected total demand in each time period after a disruptive event.

A. Mathematical Models

In this section, two variations on a mixed integer mathematical model are presented to solve the infrastructure network restoration problem. In the Binary Active model, we assume that each disrupted link remains inoperable until the related recovery process is completed. The decision variables for the Binary Active model are found in Table I. In certain realistic case studies, such as transportation networks, disrupted links can be partially operable during their recovery process. The Proportional Active model, the decision variables for which are found in Table II, addresses this situation where the level of operability of link (i,j) increases during its recovery process and becomes completely operational at the end of the recovery process.

TABLE I
DECISION VARIABLES IN THE BINARY ACTIVE MODEL

Notation	Type	Definition
α_{kijt}	Binary	Equals 1 if the recovery process of link (i,j) is completed by k work crews at time t, 0 otherwise
β_{ijt}	Binary	Equals 1 if link (i,j) is operational at time t, 0 otherwise
φ_{it}	Continuous	Cumulative flow reaching demand node i at time t
x_{ijt}	Continuous	Flow on link (i,j) at time t

TABLE II
DECISION VARIABLES IN THE PROPORTIONAL ACTIVE MODEL

Notation	Type	Definition
γ_{kijt}	Binary	Equals 1 if the recovery process of link (i,j) begins by k work crews at time t, 0 otherwise
φ_{it}	Continuous	The cumulative flow reaches to demand node i at time t
x_{ijt}	Continuous	The flow corresponding to link (i,j) at time t

1) MIP Model for Binary Active Network Restorative Capacity

$$\max \sum_{t \in T} \mu_t \Re_\varphi(t|e^j) \tag{2}$$

s.t.

$$\sum_{j:(i,j) \in A} x_{ijt} - \sum_{j:(j,i) \in A} x_{jit} \le O_i \qquad \forall i \in N_+,\ t = 1, \dots, T \tag{3}$$

$$\sum_{j:(i,j) \in A} x_{ijt} - \sum_{j:(j,i) \in A} x_{jit} = 0 \qquad \forall i \in N_=,\ t = 1, \dots, T \tag{4}$$

$$\sum_{j:(i,j) \in A} x_{ijt} - \sum_{j:(j,i) \in A} x_{jit} = -\varphi_{it} \qquad \forall i \in N_-,\ t = 1, \dots, T \tag{5}$$

$$0 \le \varphi_{it} \le b_i \qquad \forall i \in N_-, t = 1, \dots, T \tag{6}$$

$$0 \le x_{ijt} \le u_{ijt_e} \qquad \forall (i,j) \in A/A', t = 1, \dots, T \tag{7}$$

$$0 \le x_{ijt} \le \beta_{ijt} u_{ijt_e} \qquad \forall (i,j) \in A', t = 1, \dots, T \tag{8}$$

$$\sum_{k=1}^{K} \sum_{s=t}^{T} \left(1 + \left\lfloor \frac{t - (s - p_{kij} + 1)}{M} \right\rfloor\right) k \alpha_{kijs} \le L \qquad \forall (i,j) \in A', t = 1, \dots, T \tag{9}$$

$$\sum_{k\in K}\sum_{t\in T}\alpha_{kijt} \le 1 \qquad \forall (i,j)\in A' \tag{10}$$

$$\sum_{t=1}^{p_{ijk}-1}\alpha_{kijt} = 0 \qquad \forall (i,j)\in A',\ \forall k\in K \tag{11}$$

$$\beta_{ijt} - \sum_{s=1}^{t}\sum_{k\in K}\alpha_{kijs} \le 0 \qquad \forall (i,j)\in A',\ t=1,\dots,T \tag{12}$$

$$\begin{aligned} &\alpha_{kijt}, \beta_{ijt} \in \{0,1\} && \forall k\in K, \forall (i,j)\in A',\ t=1,\dots,T \\ &\varphi_{it} \ge 0 && \forall i\in N_-,\ t=1,\dots,T \end{aligned} \tag{13}$$

The objective function maximizes the resilience of the network over the horizon of the problem. We also associate weight μ_t to the resilience of the network at time t, as the importance of the resilience measure may vary over time (e.g., more rapid recovery may be achieved when earlier time periods have large weights). Eqs. (3)-(5) are network flow constraints in and out of supply nodes, transition nodes, and demand nodes, respectively. Eq. (6) ensures that the amount of delivered flow does not exceed the capacity of demand nodes. Eqs. (7) and (8) ensures that the flow of link $(i,j)\in A'$ does not exceed its (disrupted or recovered) capacity. Eqs. (9)-(12) schedule disrupted link for recovery. Eq. (9) ensures that no more than L restoration crews can work on disrupted links in each time period. None of the disrupted links receives recovery services more than once, according to Eq. (10), and no link recovery process completes before its processing time is finished with Eq. (11). Eq. (12) ensures that if link $(i,j)\in A'$ is operational at time t, then its recovery process must have been completed by that time t.

2) MIP Model for Proportional Active Network Restorative Capacity

In the Proportional Active formulation, the processing time of link $(i,j)\in A'$ is a function of: (i) the characteristics of that link, such as the level of disruption it experiences and the series of required task for its recovery, and (ii) the number of the assigned work crews to link (i,j), $f_{ijk}(t)$. This function is non-decreasing on $t=1,\dots,T$ intervals and, without loss of generality, it is integer-valued. We also assume that each recovery task should be processed without interruption.

$$\max \sum_{t\in T}\mu_t \text{Я}_\varphi(t|e^{\bar{J}}) \tag{14}$$

s.t.

Eqs. (3), (4), (5), (6), (7)

$$0 \le x_{ijt} \le u_{ijt_d} + \sum_{k\in K}\sum_{s=1}^{t}\gamma_{kijs} f_{kij(t-s)}(u_{ijt_e} - u_{ijt_d}) \qquad \forall (i,j)\in A', t=1,\dots,T \tag{15}$$

$$\sum_{k=1}^{K}\sum_{s=1}^{t}\left(1+\left\lfloor\frac{(s+p_{kij}-1)-t}{M}\right\rfloor\right)k\gamma_{kijs} \le L \qquad \forall (i,j)\in A',\ t=1,\dots,T \tag{16}$$

$$\sum_{k\in K}\sum_{t\in T}\gamma_{kijs} \le 1 \qquad \forall (i,j)\in A' \tag{17}$$

$$\sum_{t=T-p_{kij}+1}^{T}\gamma_{kijt} = 0 \qquad \forall (i,j)\in A'\ k=1,\dots,K \tag{18}$$

$$\gamma_{kijt}\in\{0,1\},\ \varphi_{it}\ge 0 \qquad \begin{matrix}\forall k\in K, \forall (i,j)\in A' \\ t=1,\dots,T,\ \forall i\in N_-\end{matrix} \tag{19}$$

Eq. (14) calculates the improvement on each disrupted link $(i,j)\in A'$ recovery process as an increase in its capacity while assuring the flow on link (i,j) does not exceed its capacity. Eqs. (15)-(17) schedule disrupted link for recovery. Eq. (16) ensures that no more than L work crews can work on disrupted links in each time period. Eq. (17) requires that the allocation of work crews is only made once for each disrupted link. No link recovery process starts if its processing time takes longer than the restoration horizon, as in Eq. (18).

The proposed formulations are applicable to various infrastructure networks, such as transportation and supply chains. However, to prove the applicability of the proposed model to power grid network it is required to update the formulation to capture the electric power flows computed according to circuit laws, which generally cannot be controlled individually by decision makers[4]. Similar to Nurre et al.[5], we apply the DC model which is a linear approximation commonly used to model the operations of power network infrastructure. The linearized approximations have been justified using traditional engineering assumptions that under "normal" operating conditions, voltage magnitudes do not significantly deviate from nominal values and phase differences are "small"[33]. To address this problem, we consider that, after the failure of components and the disconnection of overloaded components, the power system reaches to a stable state, and the model formulation is used to dispatch the power flow over the residual network. In fact, the recovery process discussed in the appendix is not intended to capture the operations of the power grid. Rather, considering the recovery of each disrupted component, it calculates the performance of the residual network iteratively and plans the restoration accordingly. The system is then dispatched for "normal" conditions using the undisrupted elements. We also incorporate cascading failure effects in early time periods after disruptions into the proposed models. Then, we employ a combined algorithm from Soltan et al.[34] and Bienstock[35] to control the disruptions caused by imbalanced supply-demand correlation (see the Appendix for details). The cascading failure evolution algorithm[34] also uses the DC approximation to calculate the network flows and prevent the violation capacity after the cascading failures. Our focus is not on the effect of cascading failures and on their control. However, applying a cascading failures control algorithm immediately after a disruptive event provides a realistic disrupted network for implementation into and testing the proposed restoration and resource allocation formulations, which is our focus. To limit the approximation errors during the deployment of this formulation on real-world systems, the AC relations can be applied in place of DC approximations[33].

III. Illustrative Examples Derived from the 400 kV French Power Transmission Network

The two proposed models are illustrated with reference to several test instances derived from the 400-kV electric power transmission network of France. The transmission network[36], depicted in Fig. 2 is the power network containing 171 nodes, including 26 generators (i.e., 26 supply nodes), 145 distributors (i.e., demand nodes), and 220 transmission lines.

To test realistic disaster areas possibly affected by realistic disruptions (e.g., Hurricane Katrina led to devastation on the U.S. gulf coast approximately half the size of Sweden[37]), we consider a hypothetically significant disruptive event (e.g., an earthquake) impacting 94 of 220 transmission lines (48%). Knowing that such a disruption would affect a geographically limited area, the disruptions are distributed randomly among the network components to evaluate the ability and behavior of the models in solving various disrupted component scenarios. The capacity of each transmission line is about 5190 MW and the total delivered power flow is 84988 MW in the nominal operating conditions. Other modified versions of disrupted transmission networks are used by Alipour et al.[38] and Fang et al.[26]. We employ different network structures to evaluate the applicability of the two proposed models. Scale-free and small-world networks are generated according to Barabasi-Albert[39] and Watts-Strogatz[40] models, respectively, based on the data describing the 400-kV French transmission network. A small-world network refers to a type of mathematical graph in which the distance between two random nodes grows slowly, proportionally to the logarithm of the number of the nodes, while at the same time the level of clustering in that corresponding network is not small[40]. These networks resemble many power grid networks and networks of how infectious disease spreads. For a scale-free network, the degree distribution follows a power law. That is, the portion of nodes having $\bar{k}$ connections to other nodes is $\bar{k}^{-\gamma}$, where γ is a parameter in the rage of (2,3)[39]. These networks resemble airline networks in the US, as well as the physical structure of the Internet and the world wide web.

The small-world and scale-free networks are not spatially embedded networks, therefore their links overlap, and the definition of series reactance loses its meaning. To mitigate this issue, we consider the generated small-world and scale-free networks as simple supply-demand networks. For generated small-world and scale-free instances, as we do not have any information about the series reactance of the lines, we need to exclude the DC flow linear approximation constraint presented by Bienstock and Mattia[4] from the model formulation when applied to these network structures. The average capacity of the lines of each network instance is chosen so that all demand nodes are satisfied.

For scale-free networks, we use preferential attachment as the growth mechanism for developing network structure for the test instances. In preferential attachment mechanism, the probability $P(i)$ that a node $i \in N$ gets a new link to another node is proportional to a positive function, A_{h_i}, of its current degree. Based on Barabasi-Albert model, $A_{h_i} = A_h$ is assumed to be a log-linear form of h^{α}, where $\alpha > 0$ is the exponent attachment[41]. The data are also generated from the 400-kV French transmission network topology with 171 nodes. Without altering the number of nodes, we vary the attachment exponent from 0.002 to 1. Changing the exponent attachment, we produce new network instances using the same number of nodes (i.e., supply, demand, and transmission nodes) with different numbers of lines and topological structure through which the disruptions are distributed in a random order.

Note that if $\alpha < 1$ (the sub-linear case), then the degree distribution is going to be a stretched exponential, while in the case of $\alpha > 1$ (super-linear case), one node will attain all the incoming links. Eventually, the power law distribution is presented only when $\alpha = 1$, linear case[41]. We alter the power of preferential attachment, which enables nodes with the higher degree to have a higher chance of grabbing new links added to the network, from 0.002 to 1.8, where 1 represents linear preferential attachment.

For small-world networks, the data are randomly generated with the same amount of supply and demand as the 400kV French transmission network data set[36], with 171 nodes and the same number of generators and distributors randomly allocated to the nodes. The capacities of lines are chosen to enable the network to satisfy all demand nodes in its undisrupted state with the minimum level of network redundancy. Without altering the number of nodes, we rewire each link with probability p from 1 to 0.001 and produce a new instance with different number of links and topological structure through which the disruptions are distributed in a random order, $p = 0$ represents a regular ring lattice network, $p = 1$ represents a complete random network, and $0 < p < 1$ represents a small-world networks.

Each generated network may have a different number of links out of which 48% are disrupted. It is assumed that 14 work crews are deployed to recover disrupted links, and at most seven crews can be assigned to a disrupted link at the same time. The restoration times for disrupted links vary between 1 to 12 periods depending on the characteristics of the link, the level of damage it experienced, and the number of assigned work crews.

We have run our computational experiment on a 64-bit Core™ i7-7500U CPU computer. We set a limit of 3600 seconds for all the instances and tested whether the proposed formulation solved them in this time limit or not. Each run was terminated before 3600 s if the optimality gap fell below 0.2% for the Proportional Active model. Python 2.7.10 is used for modeling, and Gurobi 7.0.2 is used to solve both models. The time horizon $T_{\max}$ is 60 periods (hours), which corresponds to six 10-hours work shifts.

A. Computational Testing on Scale-Free Networks

Table III presents the result of Binary Active and Proportional Active models for 17 scale-free network test instances with different exponent attachment value, $\alpha > 0, \alpha \in [0.002,1.8]$. The exponent attachment value, the capacity of links, and the total number of active links are shown in the first, second, and third columns respectively. For both models, Table III provides (i) Makespan, or the minimum recovery time required for an infrastructure network to reach to the maximum level of resilience, (ii) %Gap, the optimality gap for the obtained solution, and (iii) the CPU time required for the computation of the solutions. Restoration is depicted with Fig. 3 and Fig. 4

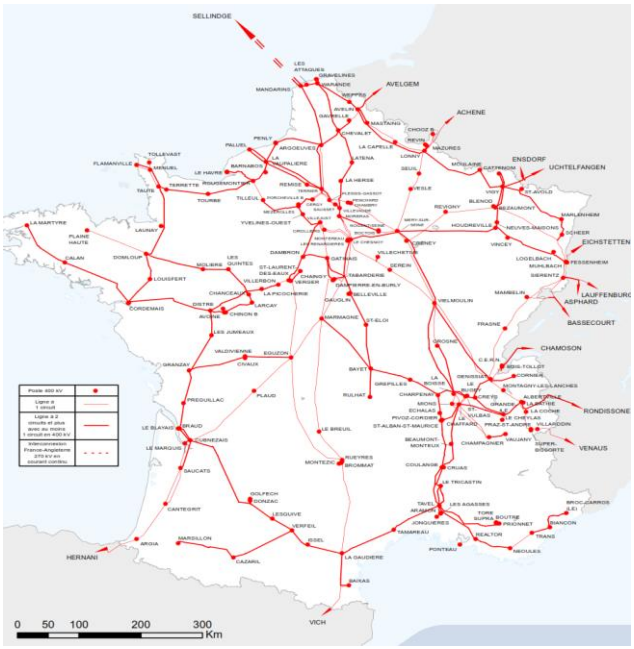

Fig. 2. The 400 kV French power transmission network[36].

Table III demonstrates that the two models can be solved within 0.6% of the optimal solution. The Proportional Active formulation recovers networks in shorter time horizons and with a lower optimality gap. As expected, Fig. 4 demonstrates that in the Proportional Active model the networks with attachment $\alpha \geq 1$ display a great tolerance against catastrophic events, as they contain highly connected nodes, which form redundant paths and support connectivity. However, the increase in the number of high degree hubs in these networks results in them being potentially highly vulnerable to malevolent attacks. In this paper, we consider natural disruptions, but intentional attacks could remove a set of more significant components that could more substantially damage the network. It is also concluded from with Fig. 3 and Fig. 4 that the higher exponent attachment α provides relatively more uniform slope and present higher resilience value in any specific time horizon.

B. Computational Testing on Small-World Networks

Table IV represents the results of the Binary Active model and Proportional Active model, respectively, for 20 small-world networks test instances with different rewiring probability scenarios. The rewiring probability and its related clustering coefficient, $C(p)$, and mean path length, $L(p)$ before the occurrence of a disruptive event, are shown in the first, second, and third columns, respectively. The fourth and fifth columns display the capacity of links and the number of links respectively. The average capacity of links changes when we change p so as to prevent flows from being rerouted through paths with redundant capacity, though rerouting is not a focus of this work. The makespan column provides the recovery time of best feasible solution, and the %Gap column provides the optimality gap for the obtained solution. The last column reports the CPU time required for computation of the solutions.

Table IV demonstrates that the Binary Active model can be solved within 0.6% of the optimal solution, and the makespan of restorative efforts increases as the rewiring probability decreases. As expected, when rewiring probability is low, the nodes that are nearby are connected (i.e., local connections), and the clustering coefficient is high as well. Although the transitivity is high, some nodes may have long distance connection which simply means it takes a long chain of connection to reach from those nodes to some others. Note that path length counts each link as length one. Fig. 5 and Fig. 6 illustrate the recovery process for Binary and Proportional formulations, where the curves associated with p =1.0, 0.6, and 0.1 represent the restorative efforts for networks with random model characteristics, curves associated with p =0.07, 0.04, and 0.01 represent networks with small-world properties, and curves associated with $p = 0.008$, 0.004, and 0.001 represent networks model characteristics. For $p \geq 0.1$, the restoration process starts from a lower level of network resilience, suggesting that these networks are more initially vulnerable to random disruptions. By increasing the rewiring probability, p, results indicate a higher percentage of recovery in a specific time horizon. The diagrams associated with $p \leq 0.008$ indicate smooth progress in the network resilience. The slope of resilience measure varies for different rewiring probabilities values in networks with rewiring probability $p \in [0.09,0.01]$, displaying much steeper recovery in the beginning for higher rewiring probabilities ($p \geq 0.06$) and more uniform progress for lower rewiring probabilities. This case study suggests that a higher cluster coefficient results in a smoother trajectory of improvement in the resilience measure. As Fig. 5 and Fig. 6 show, the makespan of restoration efforts related to different rewiring probabilities noticeably decreases when the Proportional Active model is employed. Unlike the Binary Active model, altering the rewiring probability does not significantly affect the makespan. According to Fig. 6, the trajectory of restoration for networks with different rewiring probabilities is illustrated as concave upward graphs with the uniform slope. From curves with $p \leq 0.07$, we can conclude that restoration efforts resulting from the Proportional Active model lead to more uniform restoration curves. Fig. 6 also demonstrates that higher $C(p)/C(0)$ result in less affected networks in the aftermath of a disruptive event for $p < 0.07$, suggesting that networks with lattice characteristics are less vulnerable to random disruptions. Finally, we see steeper slope of resilience enhancement in the beginning for higher rewiring probabilities ($p \geq 0.06$) and more robust networks with more uniform progress for lower rewiring probabilities ($p < 0.06$).

TABLE III
BINARY AND PROPORTIONAL ACTIVE MODEL COMPUTATIONAL RESULTS FOR SCALE FREE NETWORKS

	Link	No. of	Binary Active model			Proportional Active model		
α	capacity	links	Makespan (h)	%Gap	CPU time (s)	Makespan (h)	%Gap	CPU time (s)
0.002	13488	170	45	0.54	3600	33	0.14	3425
0.008	9375	170	43	0.41	3600	32	0.17	3266
0.02	9795	171	46	0.53	3600	31	0.19	3210
0.08	8320	170	45	0.21	3600	33	0.11	3367
0.2	16280	170	44	0.42	3600	32	0.06	3151
0.8	10480	170	44	0.21	3600	32	0.07	3207
1.2	8088	170	45	0.47	3600	33	0.02	3313
1.8	11270	171	43	0.13	3600	32	0.02	3354

TABLE IV
BINARY AND PROPORTIONAL ACTIVE COMPUTATIONAL RESULTS FOR SMALL-WORLD NETWORKS

					Binary Active model			Proportional Active model		
p	$\frac{C(p)}{C(0)}$	$\frac{L(p)}{L(0)}$	Link capacity	No. of links	Makespan (h)	%Gap	CPU time (s)	Makespan (h)	%Gap	CPU time (s)
1	0.1	< 0.04	1730	215	42	0.530	3600	32	0.253	3600
0.6	0.18	0.04	1350	237	42	0.410	3600	32	0.200	3600
0.1	0.47	0.79	1350	232	44	0.510	3600	35	0.200	3600
0.06	0.53	1.16	1015	289	44	0.343	3600	32	0.380	3600
0.01	0.62	3.81	1015	340	47	0.556	3600	29	0.406	3600
0.006	0.63	5.32	900	327	46	0.510	3600	33	0.204	3600
0.001	0.4	9.96	1015	338	54	0.345	3600	34	0.402	3600

To evaluate the tolerance and behavior of both proposed models to large disruptions resulting from any number of catastrophic events and malevolent attacks, we deactivate 40% of network links (around 68 links), either partially or completely. Considering the number of crews assigned to each disrupted link as a variable increases the complexity of the problem, regardless of the level of network disruption. Therefore, the computational results are obtained within 0.6% in the given CPU time. In cases where 7% of components are disrupted (comparable to an earthquake of magnitude 6 [Gonzalez et al. 2016a] to 16% (comparable to an earthquake of magnitude 9), the average optimality gap and solution time obtained from solving scale-free network instances are 0.025% and 7.23 seconds, respectively, for the Binary Active model, and 0.016% and 5.08 seconds, respectively, for the Proportional Active model. For small-world network instances, the average optimality gap is 0.029% and average solution time is 12.46 seconds for the Binary Active model, and for the Proportional Active model, 0.019% and 13.29 seconds, respectively.

C. *Computational Testing on the 400 kV French Transmission Network*

Fig. 7 and Fig. 8 compare the Binary Active and Proportional Active formulations for the actual 400 kV French transmission network topology as shown in Fig. 2. Although the Proportional Active formulation may only be applicable to redundant lines and components and not to all disrupted lines in the 400 kV French transmission network, it is of interest to study the behavior of both Proportional and Binary Active formulations for a real data set. We examine the effect of the two weights: (i) $w_i, i \in N_-$, for weighting the importance of demand nodes, where demand nodes located in highly populated areas are considered a higher priority relative to other demand nodes, and (ii) $\mu_t, t \in \{1, \dots, T\}$, for weighting network performance for each time period.

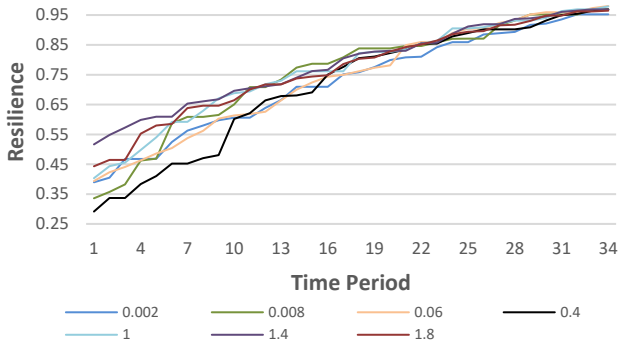

Fig. 3. Trajectory of the resilience measure for the Binary Active model applied to scale-free networks (for select values of α).

We update Eq. (1) to incorporate weights w_i in models in Eq. (20). Each takes on a constant value (where all time periods and demand nodes are weighted equally) or a scaled value (where weights are allowed to reflect importance).

$$Я_\varphi(t|e^j) = \frac{\sum_{i\in N_-} w_i\varphi_{it} - \sum_{i\in N_-} w_i\varphi_{it_d}}{\sum_{i\in N_-} w_i\varphi_{it_e} - \sum_{i\in N_-} w_i\varphi_{it_d}} \quad (20)$$

In Table V, Column 1 shows the possible combination of weighting scenarios. When μ_t is scaled, preference is given to earlier time periods. When w_i is scaled, preference is given to demand nodes in more populated areas. Remaining columns show the makespan, optimality gap, and CPU time for both models. According to Table V, both models can be solved at most within 0.7% of the optimal solution. The Proportional Active formulation results in full network performance recovery in a shorter time horizon.

TABLE V
COMPUTATIONAL RESULTS FOR THE 400-KV FRENCH TRANSMISSION NETWORK EXAMPLES (CONSIDERING CASCADING FAILURES)

	Binary Active model			Proportional Active model		
	Makespan (h)	%Gap	CPU time (s)	Makespan (h)	%Gap	CPU time (s)
w_i: constant, μ_t: constant	39	0.32	1800	35	0.70	1800
w_i: scaled, μ_t: constant	40	0.23	1800	35	0.59	1600
w_i: constant, μ_t: scaled	43	0.32	1800	38	0.66	1180
w_i: scaled, μ_t: scaled	47	0.70	1800	40	0.45	1540

TABLE VI
COMPUTATIONAL RESULTS FOR THE 400-KV FRENCH TRANSMISSION NETWORK EXAMPLES (WITHOUT CASCADING FAILURES)

	Binary Active model			Proportional Active model		
	Makespan (h)	%Gap	CPU time (s)	Makespan (h)	%Gap	CPU time (s)
w_i: constant, μ_t: constant	29	0.13	313	31	0.11	250
w_i: scaled, μ_t: constant	30	0.18	352	31	0.15	240
w_i: constant, μ_t: scaled	26	0.13	334	34	0.13	364
w_i: scaled, μ_t: scaled	31	0.15	345	36	0.14	343

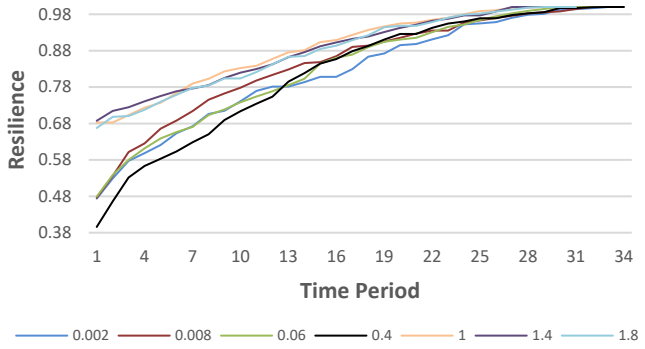

Fig. 4. Trajectory of the resilience measure for the Proportional Active model applied to scale-free networks (for select values of α).

Note that scaled μ_t may not result in a shorter recovery time horizon, though it results in a higher value of network resilience in a specific time horizon in comparison to other scenarios, as shown in Fig. 7 and Fig. 8. As expected, scaled w_i prioritizes distributers located in more populated areas to be recovered. This scenario may not lead to a shorter recovery time horizon as the prioritized distributors may be supplied via paths that do not share disrupted links with other paths in the network. Regarding the fourth scenario, where both weights are enacted, incorporating scaled μ_t may lead to more aggregate flow reaching to demand nodes in each time period, which may conflict with scaled w_i as it favors satisfying prioritized demand nodes. As such, the model restores the links that not do not carry a high percentage of accumulated network flow. Fig. 7 and Fig. 8 indicate that employing the fourth scenario does not lead to satisfying all prioritized distributers (using scaled w_i) nor to a higher value of network resilience in a specific time horizon (using scaled μ_t), a counterintuitive result.

We also analyze the restorative capacity formulation in the absence of cascading failures, Fig. 9 and Fig. 10. According to the results shown in Table VI, both models solved to within 0.18% of the optimal solution in less computational time, and both are more robust to disruption (i.e., the levels of resilience related to both models in the aftermath of the disruptions are higher than the conditions where cascading failures are considered in the corresponding models).

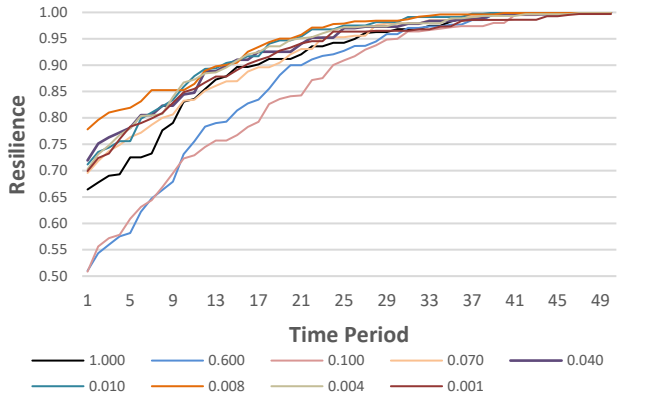

Fig. 5. Trajectory of the resilience measure for the Binary Active model applied to small-world networks (for select values of p).

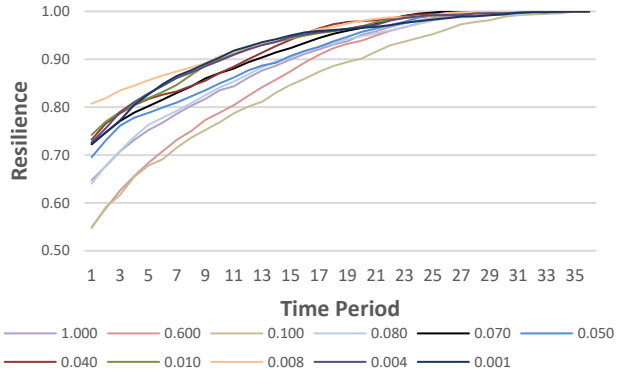

Fig. 6. Trajectory of the resilience measure for the Proportional Active model applied to small-world networks (for select values of p).

This is because, according to Algorithm 1 (shown in Appendix A), in the aftermath of a disruptive event, the difference between the voltage in generators and distributers may bring several operational links to carry redirected flow that is greater than their capacity. This overload flow causes failures

among operational links and increases the level of network disruption in a very short time period (e.g., 5 to 10 seconds). Therefore, both model formulations have to restore the network starting from a lower level of resilience.

That is, the total restoration time of the network, as well as the solution time, for the Binary and Proportional Active formulations increase considerably when considering cascading failures. Again, in cases where we disrupt 7% to 16% percent of network components, we reach an average optimality gap of 0.024% in an average solution time of 10.08 seconds for the Binary Active model, and average optimality gap of 0.014% in an average solution time of 8.05 seconds for the Proportional Active model.

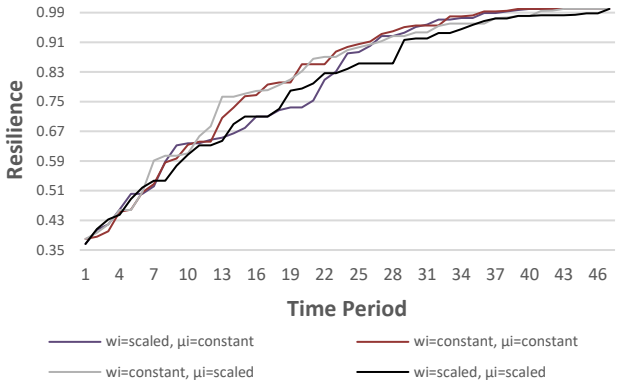

Fig. 7. Trajectory of the resilience measure for the Binary Active model applied to the 400-kV French transmission network (with cascading failures).

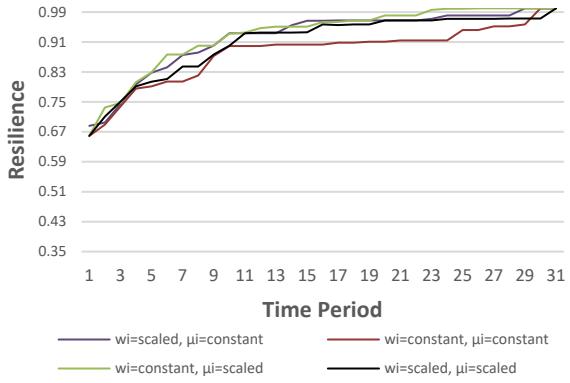

Fig. 8. Trajectory of the resilience measure for the Binary Active model applied to the 400-kV French transmission network (without cascading failures).

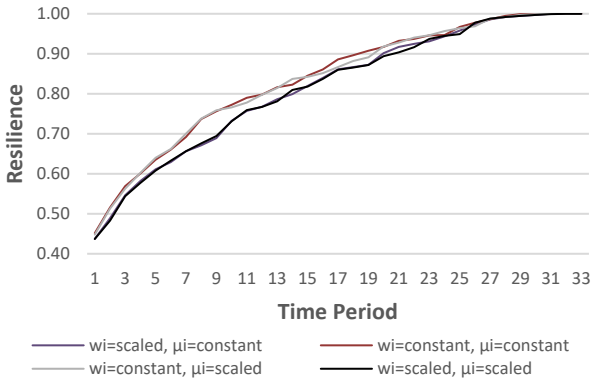

Fig. 9. Trajectory of the resilience measure for the Proportional Active model applied to the 400-kV French transmission network (with cascading failures).

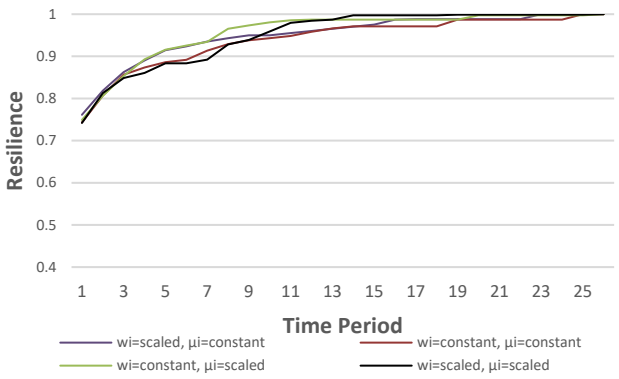

Fig. 10. Trajectory of the resilience measure for the Proportional Active model applied to the 400-kV French transmission network (without cascading failures).

IV. Concluding Remarks

This research is an attempt to explore formulations for enhancing restorative capacity that can be used in the recovery efforts of an infrastructure network after a disruptive event. Many complex networks arisen in nature or man-made environment can be represented by their scale-free and small-world properties, which are highly heterogeneous in their connectivity pattern. From scale-free and small-world networks to lattice and random networks, this problem is general enough to be applicable to a wide variety of infrastructure networks. Two formulations are proposed: (i) one that assumes that disrupted components cannot play a role in a network performance unless they are recovered completely (e.g., railway network), which we refer to as a *Binary Active* model, and (ii) one that assume that we can alter the restoration process by assuming partially recovered network components as proportionally operational (e.g., road networks), which we refer to as a *Proportional Active* model.

Although the Proportional Active model may not be always applicable on power networks, its implementation on highway networks, physical structure of internet networks is of a great significance. Proportional Active model is also applicable to some cases where, along with restoring the main power lines, temporary, and emergency lines are installed and used to satisfy at least a portion of demands. Apart from that, for expanding the evaluation of the Proportional Active formulation and for simplicity, we assume that the restoration process has a sufficiently long time horizon where there can be enough time for installation of temporary lines, particularly for severely damaged network components. Furthermore, this model is also applicable when redundant components are installed to perform the same task (e.g., parallel power lines and transformers).

The proposed formulations are path-based scheduling models that accomplish the restorative capacity goals while providing the connectivity of suppliers to demand nodes in the network during the restoration process. Solving models on 34 realistic size networks with different structures, we show that both models can produce solutions that are within 0.7% above the best possible solution in one hour of computation time. This work proposes a model that can be used following a disruptive event to restore infrastructure networks to some desired level of resilience while optimizing the restoration process aligned with the decision makers policies. The model

not only schedules work crews to restore disrupted components, but also determines where work crews should originate from, given a set of candidate locations. The proposed optimization model considers the physical interdependency between the infrastructure networks as well as the geographical interdependency when allowing work crews from different infrastructure networks to be stationed at the same established facilities.

The contributions of this paper lie in: (i) the flexibility of the number of assigned crew to each disrupted link, (ii) the Proportional Active model formulation, and (iii) the applicability of both proposed formulations on different network structures. The first contribution allows the number of restoration crews assigned to each disrupted link to differ from one link to another, so that the models are flexible enough to attain the maximum level of resilience in each time period. The second contribution incorporates each link under the restoration process as partially operational in the network. Results suggest that adopting a Proportional Active in appropriate network situations can alter tactical restoration scheduling and consequently enhance the recovery process. The third contribution studies the behavior of both formulations through different network structure (e.g., lattice, small-world, scale-free, and random networks) with various characteristics (e.g., exponent attachment, α, for scale-free networks and rewiring probabilities, p, for small-world network). Note that while reaching 0.7% of optimality is likely sufficient for such problems, an hour-long solution time may not be sufficient for decision making purposes after a disruption where good solutions are needed quickly.

As such, future work will explore heuristic methods to solve, especially larger network problems. Other future explorations include (i) the incorporation of the practical concern of work crew vehicle routing, (ii) the interdependence of infrastructure networks with each other, and (iii) the effects of network recovery not only on the network itself but on any broader socioeconomic impacts a disruption may cause. Due to the complexity of the mathematical models, the effects of such concepts as generator black start, generator ramping, and network maneuvering are not considered in the proposed formulations. An important direction for the future research is to propose an algorithm whereby we obtain the near optimal solution in a timely manner when such concepts are added to the formulation.

REFERENCES

[1] White House, Presidential Policy Directive 21 -- Critical Infrastructure Security and Resilience. Office of the Press Secretary: Washington, DC, 2013.

[2] White House, Presidential Policy Directive 8 – National Preparedness. Office of the Press Secretary: Washington, DC, 2011.

[3] S. Hosseini, K. Barker, and J. E. Ramirez-Marquez, "A review of definitions and measures of system resilience," *Reliability Engineering and System Safety*, vol. 145, pp. 47-61, 2016.

[4] D. Bienstock and S. Mattia, "Using mixed-integer programming to solve power grid blackout problems," *Discrete Optimization*, vol. 4, no. 1, pp. 115-141, 2007.

[5] S. G. Nurre, B. Cavdaroglu, J. E. Mitchell, and T. C. Sharkey, "Restoring infrastructure systems: An integrated network design and scheduling (INDS) problem," *European Journal of Operational Research*, vol. 223, no. 3, pp. 794-806, 2012.

[6] H. Baroud, K. Barker, and J. E. Ramirez-Marquez, "Importance measures for inland waterway network resilience," *Transportation Research Part E: Logistics and Transportation Review*, vol. 62, pp. 55-67, 2014.

[7] C. Nan and G. Sansavini, "A quantitative method for assessing resilience of interdependent infrastructures," *Reliability Engineering and System Safety*, vol. 157, pp. 35-53, 2017.

[8] K. Magis, "Community resilience: An indicator of social sustainability," *Society and Natural Resources*, vol. 23, pp. 401-416, 2010.

[9] D. P. Aldrich, *Building Resilience: Social Capital in Post-disaster Recovery*. Chicago, IL: University of Chicago Press, 2012.

[10] C. Béné, R. G. Wood, A. Newsham, and M. Davies, "Resilience: New Utopia or New Tyranny? Reflection about the potentials and limits of the concept of resilience in relation to vulnerability reduction programs. Brighton, UK: Institute for Development Studies, 2012.

[11] T. Frankenberger, M. Mueller, T. Spangler, S. Alexander, Community resilience: Conceptual framework and measurement feed the future learning agenda. Rockville, MD: Westat, 2013.

[12] M. Çelik, Ö. Ergun, and P. Keskinocak, "The post-disaster debris clearance problem under incomplete information. *Operations Research*, vol. 63, no. 1, pp. 65-85, 2015.

[13] *Sustainable and Resilient Infrastructure*, vol. 2, no. 2, pp. 59-67, 2017.

[14] D. Henry and J. E. Ramirez-Marquez, "Generic metrics and quantitative approaches for system resilience as a function of time," *Reliability Engineering and System Safety*, 99, pp. 114-122, 2012.

[15] K. Barker, J. E. Ramirez-Marquez, and C. M. Rocco, "Resilience-based network component importance measures," *Reliability Engineering and System Safety*, vol. 117, pp. 89-97, 2013.

[16] R. Pant, K. Barker, J. E. Ramirez-Marquez, and C. M. Rocco, "Stochastic measures of resilience and their application to container terminals," *Computers and Industrial Engineering*, vol. 70, pp. 183-194, 2014.

[17] E. D. Vugrin and R. C. Camphouse, "Infrastructure resilience assessment through control design," *International Journal of Critical Infrastructure*, vol. 7, no. 3, pp. 240-260, 2011.

[18] S. Hosseini and K. Barker, "A Bayesian network model for resilience-based supplier selection," *International Journal of Production Economics*, vol. 180, pp. 68-87, 2016.

[19] M. Kasaei and F. S. Salman, "Arc routing problems to restore connectivity of a road network," *Transportation Research Part E: Logistics and Transportation*, vol. 95, pp. 177-206, 2016.

[20] A. M. Anaya-Arenas, J. Renaud, and A. Ruiz, "Relief distribution networks: A systematic review," *Annals of Operations Research*, vol. 223, no. 1, pp. 53-79, 2014.

[21] L. Özdamar and M. A. Ertem, "Models, solutions and enabling technologies in humanitarian logistics," *European Journal of Operational Research*, vol. 244, no. 1, pp. 55-65, 2015.

[22] D. T. Aksu and L. Ozdamar, "A mathematical model for post-disaster road restoration: Enabling accessibility and evacuation," *Transportation Research Part E: Logistics and Transportation*, vol. 61, pp. 56-67, 2014.

[23] Y. P. Fang and G. Sansavini, "Optimizing power system investments and resilience against attacks," *Reliability Engineering and System Safety,* vol. 159, pp. 161-173, 2017.

[24] L. Chang and Z. Wu, "Performance and reliability of electrical power grids under cascading failures," *International Journal of Electrical Power & Energy Systems*, vol. 33, no. 8, pp. 1410-1419, 2011.

[25] H. Xiao and E. M. Yeh, "Cascading link failure in the power grid: A percolation-based analysis," In Communications Workshops (ICC), *2011 IEEE International Conference,* pp. 1-6, 2011.

[26] Y. P. Fang, N. Pedroni, and E. Zio, "Comparing network-centric and power flow models for the optimal allocation of link capacities in a cascade-resilient power transmission network," *IEEE Systems Journal*, vol. 11, no. 3, pp. 1632-1643, 2014.

[27] A. Arif, Z. Wang, J. Wang, and C. Chen. Power Distribution System Outage Management with Co-Optimization of Repairs, Reconfiguration, and DG Dispatch. IEEE Transactions on Smart Grid, 2017.

[28] B. Chen, C. Chen, J. Wang, and K. L. Butler-Purry. Sequential service restoration for unbalanced distribution systems and microgrids. IEEE Transactions on Power Systems, 2017.

[29] X. F. Wang and G. Chen, "Complex networks: small-world, scale-free and beyond," *IEEE Circuits and Systems Magazine*, vol. 3, no. 1, pp. 6-20, 2003.

[30] M. Ouyang, M. H. Yu, X. Z. Huang, and E. J. Luan, "Emergency response to disaster-struck scale-free network with redundant systems," *Physica A: Statistical Mechanics and its Applications*, vol. 387, no. 18, pp. 4683-4691, 2008.

[31] R. Albert, H. Jeong, and A. L. Barabási, "Error and attack tolerance of complex networks," *Nature*, vol. 406, no. 6794, pp. 378-382, 2000.
[32] R. K. Ahuja, T. L. Magnanti, and J. B. Orlin, *Network Flows: Theory, Algorithms, and Applications*, 1993.
[33] H. Nagarajan, R. Bent, P. Van Hentenryck, S. Backhaus, and E. Yamangil, "Resilient Transmission Grid Design: AC Relaxation vs. DC approximation," https://arxiv.org/abs/1703.05893.
[34] S. Soltan, D. Mazauric, and G. Zussman, "Cascading failures in power grids: analysis and algorithms," *In Proceedings of the 5th International Conference on Future Energy Systems*, pp. 195-206, 2014.
[35] D. Bienstock, "Optimal control of cascading power grid failures," *In Decision and control and European control conference (CDC-ECC)*, pp. 2166-2173, 2011.
[36] Le Réseau de Transport d'Electricité 400 kv, RTE, Paris, France, Nov. 2013. <www.rte-france.com/uploads/media/CS4_2013.pdf>.
[37] Widegren, K. 2007. Återuppbyggnaden efter orkanerna Katrina och Rita. *Swedish Institute for Growth Policy Analysis (ITPS)*, Arbetsrapport, 11.
[38] Z. Alipour, M. A. S. Monfared, and E. Zio, "Comparing topological and reliability-based vulnerability analysis of Iran power transmission network," *Journal of Risk and Reliability*, vol. 228, no. 2, pp. 139-151, 2014.
[39] A. L. Barabási and R. Albert, "Emergence of scaling in random networks," *Science*, vol. 286, no. 5439, pp. 509-512, 1999.
[40] D. J. Watts and S. H. Strogatz, "Collective dynamics of 'small-world' networks," *Nature*, vol. 393, no. 6684, pp. 440-442, 1998.
[41] T. Pham, P. Sheridan, and H. Shimodaira, "PAFit: A statistical method for measuring preferential attachment in temporal complex networks," *PloS one*, vol. 10, no. 9, art. e0137796, 2015.

APPENDIX

A. Controlling Cascading Failures in a Power Network

Although integrating DC flow approximation constraints with the proposed models prevents any violation of link capacity, in reality, an initial disruption sets off a sequence of additional disturbances in the network in a time horizon that is on the order of minutes. We implement the Cascading Failure Evolution (CFE) algorithm introduced by Soltan et al.[34]. We implement the cascading process in ten rounds, $R = 10$, and terminate the process using the termination law proposed by Bienstock[35].

Algorithm 1 – Cascading Failure Evolution (CFE)

Input: Graph $G = (V, A)$ and the set of initial disrupted links $A'_0 \subseteq A$
1: $A'^*_0 \leftarrow A'_0$ and $i \leftarrow 0$.
2: for $r = 1, \dots, R$
3: Adjust total demand to total supply within each connected island κ $\kappa \subseteq G = (V, A \backslash A'^*)$.
4: Compute the new flows $x_{ijr}(A'^*) \quad \forall (i,j) \in A \backslash A'^*$.
5: Find the set of new links $A'_{r+1} = \{(i,j) | x_{ijr}(A'^*) > u_{ijt_e}, A \backslash A'^*\}$, $A'^*_{r+1} \leftarrow A'^*_r \cup A'_{r+1}$.

Termination. (round R) If any component has overload line, proportionally decrease the demand until all flows fall into capacity range. Set $\psi_K^R = \min\{1, \max_{(i,j)\in K} |x_{ijr}(A'^*_R)| / u_{ijt_e}\}$. If $\psi_K > 1$, then any distributer in round R in each component resets its demand to b_i^R / ψ_K^R.

The input of the algorithm is the initial set of disrupted links immediately after the occurrence of a disruptive event. We assume this set as the initial optimal set of disrupted links A'^*_0. It is assumed that the flow of each link falls in its capacity range, $|x_{ijt_e}| \leq u_{ijt_e}$. After a disruptive event, some links fail and disconnect the network to $\kappa = \{1, .., K\}$ islands. Each island may have a number of generators and distributors whose total pre-disruption supply and demand were not in balance. The network still sets the total supply and demand balance in each island. However, there are not an adequate amount of capacity due to the failure of some links, and this leads to the overload of some operational links and consequently other links may fail. In each round, a set of new disrupted links $A'_{r+1} \subseteq A$ is added to the previous set to form a new set of disrupted links $A'^*_{r+1} \leftarrow A'^*_r \cup A'_{r+1}$. In the last round, the total demand in each island is adjusted to be equal to total supply of that island decreasing the level of demand (supply), referred to as the shedding/generation process[34]. We assume that the supply-demand balance is considered in each time period of the recovery process to prevent additional disruptions.

Nazanin Morshedlou is a post-doctoral scholar in the School of Industrial and Systems Engineering at the University of Oklahoma. She received a B.S degree from Sharif University of Technology in 2010, an M.S. degree from the University of Tehran in 2013, and a Ph.D. from the University of Oklahoma in 2018. Her research interests within OU's Risk-Based Systems Analytics Laboratory include the development of optimization models and algorithms to enhance response and restoration processes in complex infrastructure networks, the impact of routing problems on network resilience, and cascading failure analysis in power systems.

Kash Barker is an Associate Professor and Anadarko Petroleum Corporation Presidential Professor in the School of Industrial and Systems Engineering at the University of Oklahoma. His work broadly dealing with reliability, resilience, and economic impacts of infrastructure networks has been funded by the National Science Foundation, Department of Transportation, Department of the Navy, and Army Research Office, among others, and has resulted in over 45 refereed journal publications. He received B.S. and M.S. degrees in Industrial Engineering from the University of Oklahoma and a Ph.D. in Systems Engineering from the University of Virginia. He is an Associate Editor of *IISE Transactions* and is on the editorial board of *Risk Analysis*.

Giovanni Sansavini received his B.S. in Energy Engineering, M.A. and Ph.D degrees in Nuclear Engineering, respectively, in 2003, 2005 and 2010 from Politecnico di Milano. In 2010, as a member of the Atlantis Dual Doctoral Degree Program, he received his Ph.D. in Mechanical Engineering from Virginia Tech. He is currently an Assistant Professor of Reliability and Risk Engineering at ETH Zurich. His research focuses on the development of hybrid analytical and computational tools suitable for analyzing and simulating failure behaviors of engineered complex systems (i.e., highly integrated energy supply, energy supply with high penetrations of renewable energy sources, communication, transport, and other physically networked critical infrastructures).